

Lawrence Berkeley National Laboratory

Recent Work

Title

ORBITAL-COLLAPSE EFFECTS IN PHOTOEMISSION FROM ATOMIC Eu

Permalink

<https://escholarship.org/uc/item/0jx924zf>

Author

Becker, U.

Publication Date

1985-07-01



Lawrence Berkeley Laboratory

UNIVERSITY OF CALIFORNIA

Materials & Molecular Research Division

Submitted to Physical Review Letters

ORBITAL-COLLAPSE EFFECTS IN PHOTOEMISSION
FROM ATOMIC Eu

U. Becker, H.G. Kerkhoff, D.W. Lindle,
P.H. Kobrin, T.A. Ferrett, P.A. Heimann,
C.M. Truesdale, and D.A. Shirley

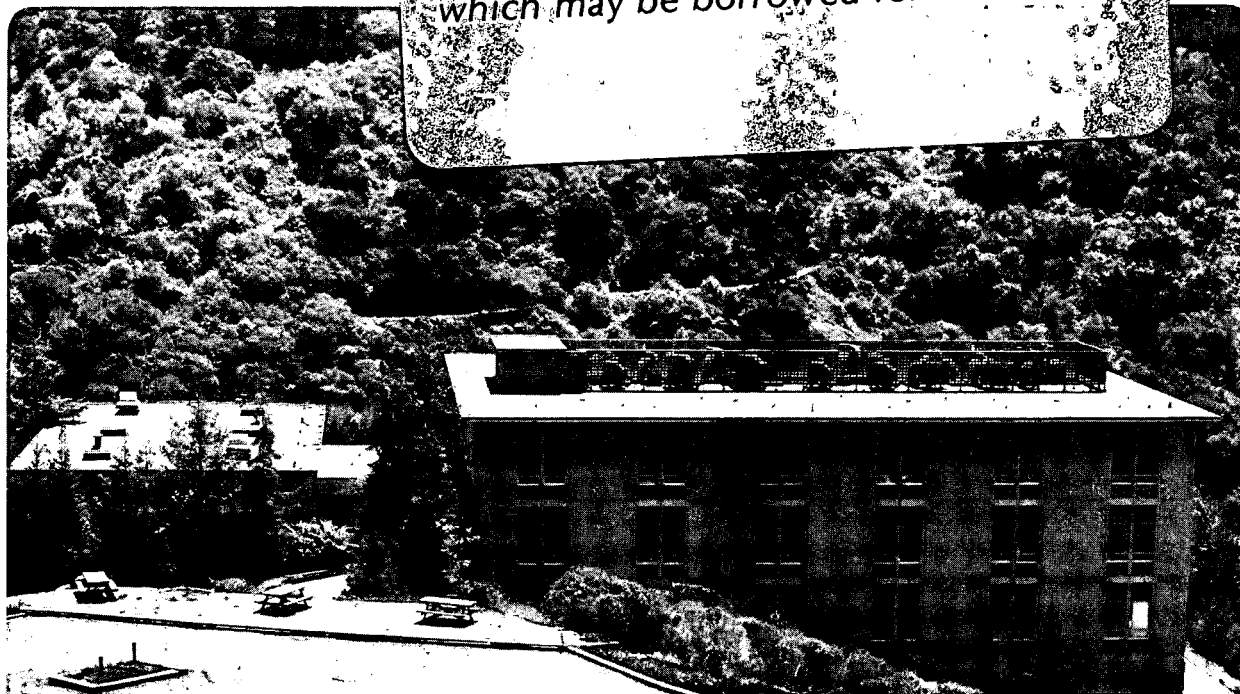
July 1985

RECEIVED
LAWRENCE
BERKELEY LABORATORY

OCT 9 1985

LIBRARY AND
DOCUMENTS SECTION

TWO-WEEK LOAN COPY
*This is a Library Circulating Copy
which may be borrowed for two weeks.*



*LBL-16066
e.2*

DISCLAIMER

This document was prepared as an account of work sponsored by the United States Government. While this document is believed to contain correct information, neither the United States Government nor any agency thereof, nor the Regents of the University of California, nor any of their employees, makes any warranty, express or implied, or assumes any legal responsibility for the accuracy, completeness, or usefulness of any information, apparatus, product, or process disclosed, or represents that its use would not infringe privately owned rights. Reference herein to any specific commercial product, process, or service by its trade name, trademark, manufacturer, or otherwise, does not necessarily constitute or imply its endorsement, recommendation, or favoring by the United States Government or any agency thereof, or the Regents of the University of California. The views and opinions of authors expressed herein do not necessarily state or reflect those of the United States Government or any agency thereof or the Regents of the University of California.

LBL-16066

Orbital-Collapse Effects in Photoemission from Atomic Eu

U. Becker and H.G. Kerkhoff

Institut für Strahlungs- und Kernphysik
Technische Universität Berlin, D-1000 Berlin 12, W. Germany,
and
Materials and Molecular Research Division
Lawrence Berkeley Laboratory
Berkeley, California 94720

D.W. Lindle, P.H. Kobrin,* T.A. Ferrett, P.A. Heimann,
C.M. Truesdale,† and D.A. Shirley

Materials and Molecular Research Division
Lawrence Berkeley Laboratory
and
Department of Chemistry
University of California
Berkeley, California 94720

Resonant photoelectron spectra of atomic Eu have been measured in the photon-energy ranges of the "4d \rightarrow 4f" (110-170 eV) and 3d \rightarrow 4f (1120-1165 eV) excitations. The "4d \rightarrow 4f" resonance data provide the first determination in a free atom of the decay channels of a "giant resonance" which peaks above its associated threshold. For both inner-shell excitations, decay to Eu⁺ main-line configurations is observed, this being the dominant deexcitation process for the "4d \rightarrow 4f" resonance. The 3d \rightarrow 4f excitations, however, are characterized by competition between the main-line decay channels and channels corresponding to highly-excited ionic states (satellites). The measured relative partial cross sections indicate that decay after 4d excitation leads predominantly to the 4f manifold, whereas several channels participate in the decay following 3d excitation. The results are interpreted with regard to orbital-collapse phenomena.

*Present address: Rockwell Science Center, PO Box 1085, Thousand Oaks, CA 91360.

†Present address: Research and Development Division, Corning Glass Works, Corning, NY 14831.

Inner-shell photoabsorption spectra of atomic transition-metal vapors exhibit "giant resonances" associated with excitations into partially occupied nd or nf subshells.¹ For the rare earths, these resonances ("4d \rightarrow 4f") have attracted increasing attention in both atomic²⁻⁶ and solid-state physics.⁷⁻¹⁷ Different theoretical approaches^{18,19} have attributed "4d \rightarrow 4f" resonances (and giant resonances in general) to an orbital-collapse effect. In some aspects, the resonance effect is similar to shape-resonance phenomena which arise from a centrifugal barrier in the effective potential for the excited electron.²⁰ Calculations^{19,21} have shown that the inner well of this potential becomes deeper as Z (or the effective charge Z_{eff}) increases. As a result, the resonances gradually move closer to and finally below the 4d threshold, as exhibited in the isonuclear sequence Ba, Ba⁺, Ba⁺⁺.⁵ Similarly, with increasing atomic number the well deepens rapidly, leading to a sudden decrease in both the energy and size of the 4f orbital as it contracts into the inner well over a certain range of Z: hence the term "collapse". This trend also can occur for the same Z if deeper-lying core electrons (e.g. 3d instead of 4d) are excited into the 4f subshell because of the accompanying increase in Z_{eff} . The so-called "4d \rightarrow 4f" resonant states²² can be considered as inner-well eigenstates with hybrid character which can behave both like a shape resonance by tunneling through the potential barrier and like a discrete (Feshbach) resonance by autoionizing into neighboring continua.

Direct determination of the decay channels of these inner-shell

resonances, obtained by photoemission studies of the rare earths, provides a very sensitive probe of the effective potential for electrons in the partially filled 4f subshell. In this Letter we report the first such measurements for atomic "4d \rightarrow 4f" and 3d \rightarrow 4f excitations. In particular we have studied resonance phenomena in Eu, an element for which the oscillator strength of the "4d \rightarrow 4f" excitation peaks above the 4d_{5/2} ionization threshold. Thus, the "4d \rightarrow 4f" data yield the first comprehensive results about the relative contributions of autoionization and electronic shape-resonance decay channels to deexcitation of atomic giant resonances. In contrast, the 3d \rightarrow 4f excitations are discrete transitions lying below their respective 3d ionization limits, thereby making Eu a good candidate for studying orbital-collapse phenomena.

The measurements were made at the Stanford Synchrotron Radiation Laboratory using a time-of-flight (TOF) electron spectrometer described elsewhere.²³ By monitoring the total photoemission intensity at 54.7° relative to the photon polarization vector, we obtained relative total-yield spectra, which allowed an internal calibration of the photon energy (± 1 eV) for the "4d \rightarrow 4f" resonance measurements by comparison with known photoabsorption data.² The 3d \rightarrow 4f energy range was calibrated with a similar uncertainty by measuring a Ne 1s \rightarrow 3p excitation spectrum. The energy levels relevant to this work are depicted in Fig. 1.

Figure 2 shows total-yield spectra of Eu taken in the photon-energy ranges of the "4d \rightarrow 4f" and 3d \rightarrow 4f excitations. Figure 3

shows photoelectron TOF spectra taken at selected photon energies. The TOF spectra in Fig. 3a were taken at $h\nu=138$ eV, on the low-energy side of the "4d \rightarrow 4f" resonance, which peaks at $h\nu=141$ eV, above the $4d_{5/2}$ threshold at 137 eV. The TOF spectra in Fig. 3b were taken at $h\nu=1126$ eV right on the peak of the $3d_{5/2} \rightarrow 4f$ resonance (top) and at $h\nu=1120$ eV (bottom). The $4d_{5/2,3/2}$ and $3d_{5/2,3/2}$ thresholds (137.5, 142.6, 1131, and 1163 eV, respectively) shown in Fig. 2 were derived from the measured photoelectron kinetic energies.

Several decay channels are available following the 3d and 4d excitations. For the "4d \rightarrow 4f" resonance, we shall consider two principal types of deexcitation paths, recognizing that their definitions are limited by our incomplete understanding of the decay dynamics of giant resonances.

- 1) the excited 4d electron experiences an enhancement (via intrachannel tunneling) similar to a shape resonance, resulting in a (main line) $\text{Eu}^+ 4d^{-1}$ photoemission final state. Connerade²⁴ has discussed this channel in the context of a shape-independent model.²⁵
- 2) the resonant state decays by autoionization (via interchannel coupling), resulting in Eu^+ configurations corresponding to main lines other than $4d^{-1}$, and their correlation and spin-flip satellites.

For the discrete 3d \rightarrow 4f resonances, pathway 1 leading to a $3d^{-1}$ final state is energetically inaccessible, and it is convenient to divide the autoionization channels (pathway 2) according to the final

ionic states produced, as follows:

- 2a) the 4f subshell to which the 3d electron was excited is involved in the decay, resulting in Eu^+ main-line configurations.²⁶
- 2b) the 4f subshell, including the excited 4f electron, remains as a spectator to the decay process, resulting in Eu^+ satellite configurations with eight 4f electrons, which we shall refer to as spectator satellites.²⁷

The differentiation of pathways 2a and 2b is possible for the $3d \rightarrow 4f$ resonances because the 3d excitation populates the discrete 4f orbital, whereas the 4d electron excited by the " $4d \rightarrow 4f$ " resonance is placed in a hybrid $\ell=3$ state (not $n=4$).

Resonant photoelectron spectroscopy provides the opportunity to measure directly the relative cross sections of the different decay channels listed above. In the " $4d \rightarrow 4f$ " resonance case, the photoelectron spectrum in Fig. 3a shows the predominance of auto-ionization (pathway 2) to the 4f final state over autoionization to the other final states observed in the spectrum. Figure 4 shows the partial cross sections for 4d, 4f, 5p, and 6s photoemission in the vicinity of the " $4d \rightarrow 4f$ " resonance. A similar result for the 4f cross section was obtained from the corresponding constant-initial-state spectrum of Eu metal.¹⁴

The 4d photoemission cross section measured above 160 eV is found to account for less than 25% of the total photoabsorption cross section. Auger electrons from decay of 4d-hole states were observed

for photon energies near the peak of the giant resonance, providing information on the near-threshold behavior of the 4d cross section. The results in Fig. 4 show that photoemission into the 4d channel (pathway 1) is less likely than decay into the 4f main-line continuum (pathway 2), confirming a calculation by Amusia et al.,²⁸ as well as indicating that the degree of "partial collapse"²⁹ of the 4f wavefunction is large. The favored exit channel for the giant resonance is apparently the super-Coster-Kronig-like (sCK) decay^{30,31} $4d^9 4f^8 \rightarrow 4d^{10} 4f^6_{ed,g}$, leaving the ion in the same final state as reached by 4f photoemission. This behavior is analogous to the decay of the $3p \rightarrow 3d$ excitation in atomic Mn.³² The importance of autoionization decay for the "4d \rightarrow 4f" resonance demonstrates that photoabsorption spectra of giant resonances are insufficient to test the shape-independent approximation:^{17,24} measurements of partial cross sections are required.

Turning to the $3d \rightarrow 4f$ excitations, the spectrum in Fig. 3b shows that several of the main-line and spectator-satellite channels are enhanced by autoionization. There is no 3d photoemission peak because the $3d_{5/2}$ resonance lies below threshold. From the binding energies and photon-energy dependences of the emitted electrons compared to the nonresonant spectrum (lower spectrum in Fig. 3b), we propose the following assignments of the peaks in the resonant spectrum. The first two peaks correspond primarily to autoionization into the 4f and 4d main lines, respectively. The third peak contains the $4d^{-2} 4f^8$ spectator satellite group and a small contribution from the 4p main

line, whereas the last two features most likely are due to spectator transitions to the $4p^{-1}4d^{-1}4f^8$ and $4s^{-1}4d^{-1}4f^8$ groups, respectively. The limited resolution of the TOF spectra is insufficient to measure quantitatively the relationship between autoionization into the main-line (pathway 2a) and spectator (pathway 2b) transitions, but it does show qualitatively the competition between the two types of decay channels.

For the $3d_{3/2} \rightarrow 4f$ excitation (TOF spectrum not shown), the $3d_{5/2}$ main-line state also can be reached by autoionization, and in fact this channel accounts for almost half of the total intensity at the $3d_{3/2} \rightarrow 4f$ resonance. We conclude that autoionization to the main $n=3,4$ photoemission final states contributes considerably to the decay of the $3d \rightarrow 4f$ excitations, especially for the $3d_{3/2}$ spin-orbit component. This result is in good agreement with theoretical predictions for La,³³ and consistent with the asymmetric line-shape of the $3d_{3/2}$ resonance in our total-yield spectrum.

In Fig. 5 we show the partial cross sections of the $4d$, $4f$, and $3d_{5/2}$ main-line channels and of the $4d^{-2}4f^8$ and $4p^{-1}4d^{-1}4f^8$ spectator satellites (the "4f peak" includes contributions from the 5s, 5p, and 6s subshells, and the satellites include some 4p and 4s main-line intensity, respectively) in the $3d \rightarrow 4f$ excitation energy range. These results show there is no specially favored decay channel, in contrast to the " $4d \rightarrow 4f$ " excitation, but rather that many open channels participate in the decay of the excited states, including significant decay of the $3d_{3/2} \rightarrow 4f$ resonance to the $3d_{5/2}$ channel.

However, enhancement of the satellites shows that autoionization via spectator transitions (pathway 2b) is competitive in the decay of a 3d hole. Our observations of decay to the $4f^{-1}$ state corroborate findings by inverse photoemission⁸ (bremsstrahlung enhancement) as well as by direct valence-band photoemission obtained recently for different rare-earth compounds.¹⁶

In conclusion we have shown that autoionization to main-line configurations is the dominant decay process for the "4d \rightarrow 4f" resonance in Eu, although this resonance exhibits some shape-resonance "character" as well. The decay of the 3d \rightarrow 4f resonances shows strong competition between autoionization to main lines and spectator satellites. The populations of the different main-line exit channels change dramatically with the quantum number of the core hole created after excitation to the 4f subshell. This quantitative difference in decay-channel cross sections may be related to the degree to which the vacancy dependence of the double-well potential (as seen very recently for molecules³⁴) and thereby the orbital-collapse effect modifies the $\ell=3$ excited-state wavefunction. The collapsed 4f wavefunction following 3d \rightarrow 4f excitation produces a strong autoionizing resonance by virtue of being localized in the inner well of the atomic potential, whereas the $\ell=3$ wavefunction populated by the "4d \rightarrow 4f" excitation may be regarded as "partially collapsed" with enough continuum character to produce some shape-resonance-like decay (pathway 1). A complete understanding of how these differing intermediate-state wavefunctions affect the different decay-channel probabilities will require further

theoretical analysis and experimental studies. Finally, we expect that the decay characteristics observed in Eu also will be found in other rare-earth elements, and that detailed study with higher resolution will yield new insights into inner-shell excitations and giant-resonance phenomena.

Acknowledgements

This work was supported by the Director, Office of Energy Research, Office of Basic Energy Sciences, Chemical Sciences Division of the U.S. Department of Energy under Contract No. DE-AC03-76SF00098. It was performed at the Stanford Synchrotron Radiation Laboratory, which is supported by the Department of Energy's Office of Basic Energy Sciences. One of us (U.B.) acknowledges funding by the Bundesministerium für Forschung und Technologie (BMFT) and another (H.G.K.) support by the Wigner foundation.

References

1. J.L. Dehmer, A.F. Starace, U. Fano, J. Sugar, and J.W. Cooper, Phys. Rev. Lett. 26, 1521 (1971); J.P. Connerade, Contemp. Phys. 19, 415 (1978).
2. M.W.D. Mansfield and J.P. Connerade, Proc. R. Soc. A 352, 125 (1976).
3. E.-R. Radtke, J. Phys. B 12, L71 (1979).
4. E.-R. Radtke, J. Phys. B 12, L77 (1979).
5. T.B. Lucatorto, T.J. McIlrath, J. Sugar, and S.M. Younger, Phys. Rev. Lett. 47, 1124 (1981).
6. R.C. Karnatak, J.M. Esteva, and J.P. Connerade, J. Phys. B 14, 4747 (1981).
7. T.M. Zimkina, V.A. Fomichev, S.A. Gribovskii, and I.I. Zhukova, Fiz. Tverd. Tela. 9, 1447 (1967); Sov. Phys. Solid State 9, 1128 (1967).
8. M.B. Chamberlain, A.F. Burr, and R.J. Liefeld, Phys. Rev. A 9, 663 (1974).
9. C. Bonelle, R.C. Karnatak, and N. Spector, J. Phys. B 10, 795 (1977).
10. W. Lenth, F. Lutz, J. Barth, G. Kalkoffen, and C. Kunz, Phys. Rev. Lett. 41, 1185 (1978).
11. J.W. Allen, L.I. Johansson, R.S. Bauer, I. Lindau, and S.B.M. Hagstrom, Phys. Rev. Lett. 41, 1499 (1978).
12. W.F. Egelhoff, G.G. Tibbets, M.H. Hecht, and I. Lindau, Phys. Rev. Lett. 46, 1071 (1981).

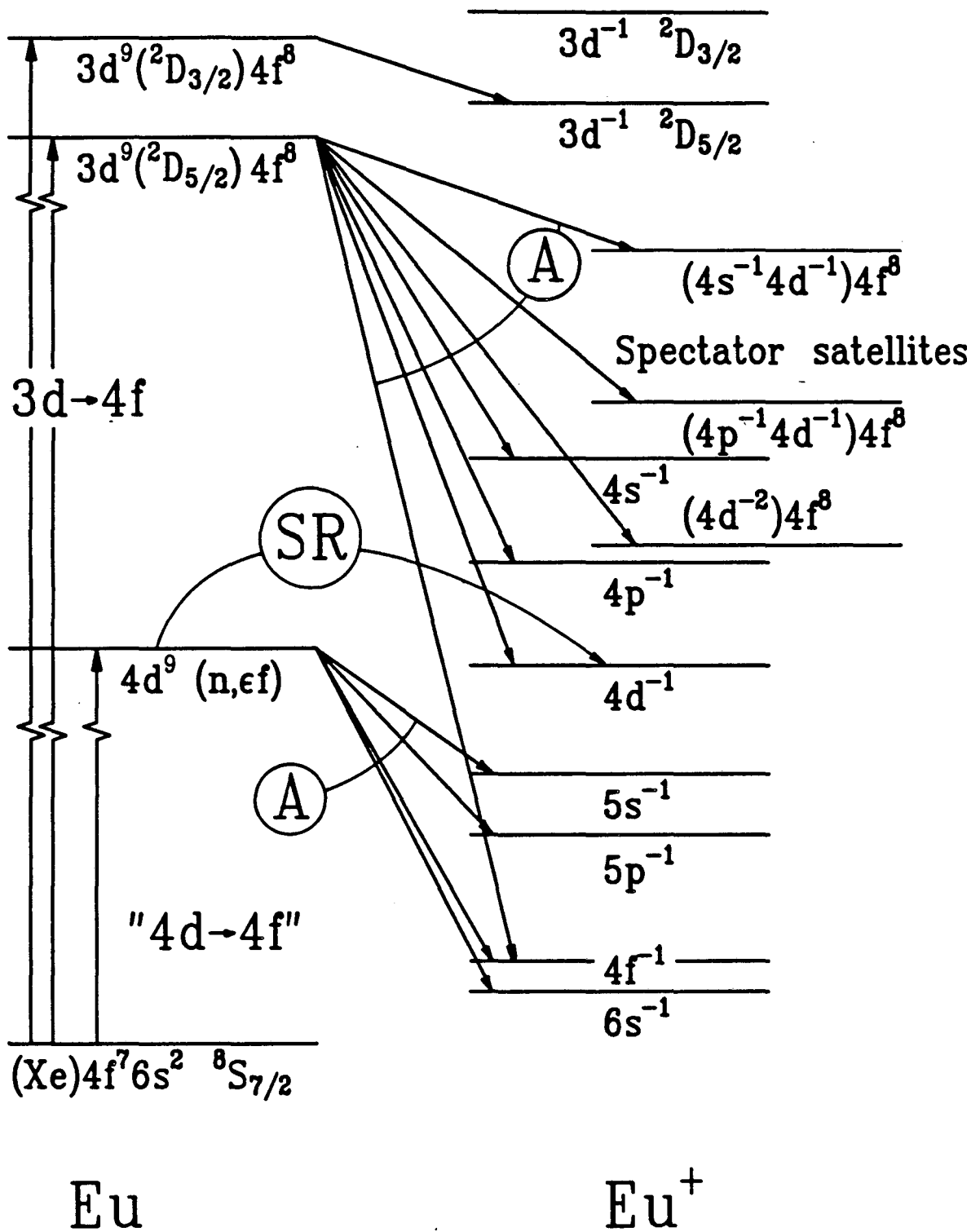
13. M.H. Hecht and I. Lindau, Phys. Rev. Lett. 47, 821 (1981).
14. F. Gerken, J. Barth, and C. Kunz, Phys. Rev. Lett. 47, 993 (1981); Proceedings of the International Conference on X-Ray and Atomic Inner-Shell Physics, Eugene, Oregon, 1982, AIP Conference Proceed. No. 94, ed. by B. Crasemann (AIP, New York, 1982).
15. G. Kaindl, G. Kalkowski, W.D. Brewer, B. Perscheid, and F. Holtzberg, J. App. Phys. 55, 1910 (1984).
16. J.W. Allen, S.J. Oh, I. Lindau, and L.I. Johansson, Phys. Rev. B 29, (1984).
17. J.P. Connerade and M. Pantelouris, J. Phys. B 17, L173 (1984).
18. K.T. Cheng and W.R. Johnson, Phys. Rev. A 28, 2820 (1983).
19. K.T. Cheng and C. Froese-Fischer, Phys. Rev. A 28, 2811 (1983).
20. M. Goeppert-Mayer, Phys. Rev. 60, 184 (1941); J.W. Cooper, Phys. Rev. Lett. 13, 762 (1964).
21. S.T. Manson and J.W. Cooper, Phys. Rev. 165, 126 (1968).
22. We use quotes here for the "4d \rightarrow 4f" resonance in recognition of the fact that the 4d \rightarrow 4f Rydberg excitation lies below the 4d threshold, whereas the oscillator strength of the so-called "4d \rightarrow 4f" giant resonance lies above threshold.¹
23. M.G. White, R.A. Rosenberg, G. Gabor, E.D. Poliakoff, G. Thornton, S. Southworth, and D.A. Shirley, Rev. Sci. Instrum. 50, 1288 (1979); P.H. Kobrin, U. Becker, S. Southworth, C.M. Truesdale, D.W. Lindle, and D.A. Shirley, Phys. Rev. A 26, 842 (1982).

24. J.P. Connerade, J. Phys. B 17, L165 (1984); see also J.R. Peterson, Y.K. Bae, and D.L. Huestis, Ninth International Conference on Atomic Physics Abstracts, Seattle (1984).
25. The shape-independent model treats giant resonances as shape-resonance phenomena which arise from strong overlap between the inner-well eigenstate and high- ℓ continuum final states at a well-defined energy.²¹ This approach yields a formula predicting a different resonance shape than a Beutler-Fano profile and which depends on the parameters of the inner well of the effective potential. Such an interpretation regards continuum giant resonances as an effect within a single channel, in contrast to autoionization which is an interchannel effect.
26. Because of the difference in spins of the electron excited to the 4f orbital and the "other" seven 4f electrons, the term symbol for the main-line configurations will vary depending on which 4f electron undergoes the decay. However, the present low-resolution results only distinguish among the different configurations.
27. Note that only final ionic states with an extra electron remaining in the 4f subshell fall under this classification, hence the name spectator satellite. Other satellites, of course, are possible, but do not have this spectator character, and therefore we include them implicitly with pathway 2a.
28. M.Y. Amusia, S.I. Sheftel, and L.V. Chernysheva, Sov. Phys. Tech. Phys. 26, 1444 (1982).

29. The term "partial collapse" is used here as a measure of the mixing between continuum and bound states that is governed by orbital collapse (see Ref. 1).
30. E.J. McGuire, J. Phys. Chem. Solids 33, 577 (1972).
31. In a different model, decay of the "4d \rightarrow 4f" excitation is described by collective oscillations. See A. Zangwill and P. Soven, Phys. Rev. Lett. 45, 204 (1980).
32. R. Bruhn, E. Schmidt, H. Schröder, and B. Sonntag, Phys. Lett. 90A, 41 (1982); P.H. Kobrin, U. Becker, C.M. Truesdale, D.W. Lindle, H.G. Kerkhoff, and D.A. Shirley, J. Electron Spectrosc. 34, 129 (1984); M.O. Krause, T.A. Carlson, and A. Fahlman, Phys. Rev. A 30, 1316 (1984).
33. F. Combet Farnoux, Phys. Rev. A 25, 287 (1982); 13th International Conf. on Physics of Electronic and Atomic Physics Abstracts, edited by J. Eichler, W. Fritsch, I.V. Hertel, N. Stotterfoht, and U. Wille (Berlin, 1983).
34. J.-H. Fock and E.E. Koch, Chem. Phys. (in press).

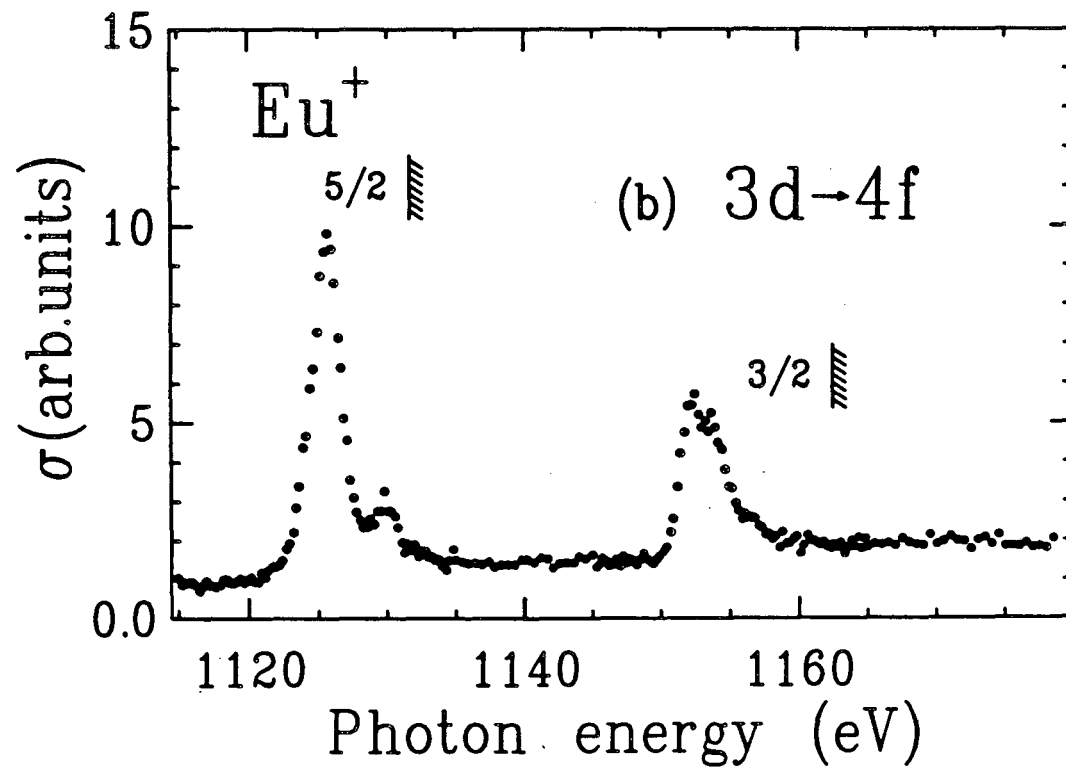
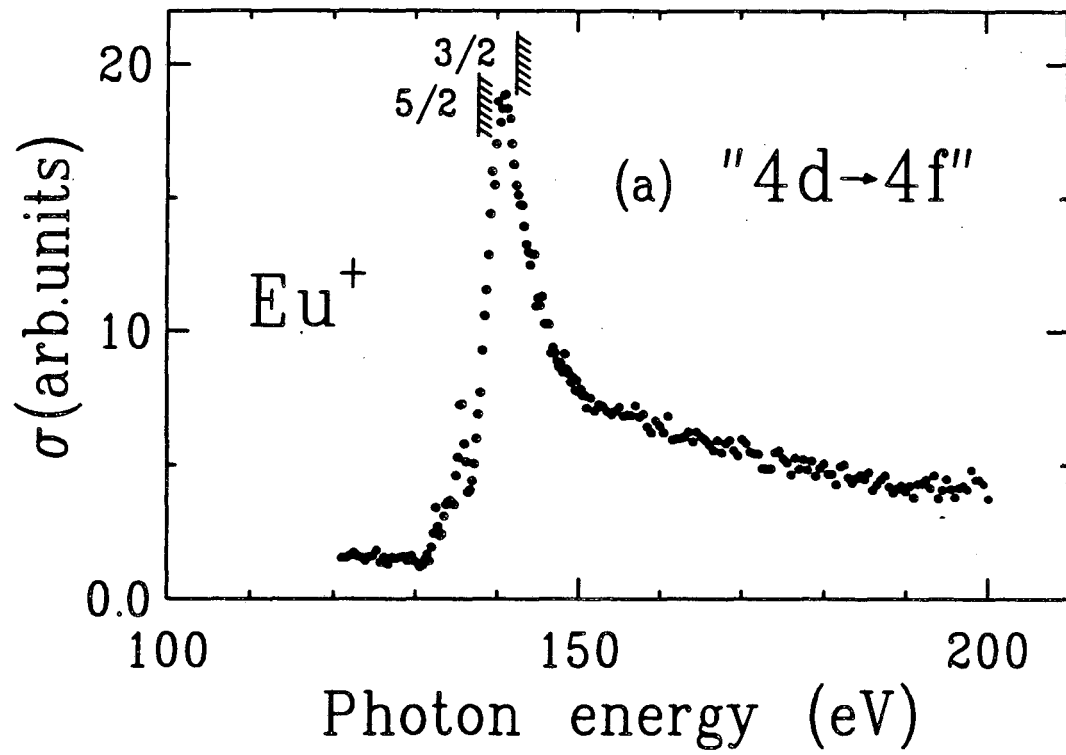
Figure Captions

- Fig. 1. Energy-level diagram of Eu, indicating the transitions studied. A = autoionization, SR = shape resonance. Some decay channels have been omitted for clarity.
- Fig. 2. Total-yield spectra of Eu in the photon-energy ranges of the (a) "4d \rightarrow 4f" and (b) 3d \rightarrow 4f resonances.
- Fig. 3. TOF photoelectron spectra of Eu vapor taken with photon energies of (a) 138 eV near the "4d \rightarrow 4f" resonance and (b) 1126 eV at the maximum of the 3d_{5/2} spin-orbit component of the 3d \rightarrow 4f resonance, compared to a nonresonant spectrum at $h\nu=1120$ eV [lower part of (b)]. The insert in (a) shows the presence of spin-flip satellites of the 4f peak.
- Fig. 4. Partial cross sections of the 4d (squares, open squares for 4d_{5/2} only), 4f (circles), 5p (diamonds), and 6s (triangles) main lines in the vicinity of the "4d \rightarrow 4f" giant resonance. The solid curves represent two-resonance fits with Beutler-Fano profiles [$q_{\text{eff}}(4f)=1.6$, $\Gamma=4.4$ eV]. The dotted line represents the shape-resonantly enhanced 4d_{5/2} cross section in the shape-independent approximation.
- Fig. 5. Partial cross sections of the 4d (triangles), 4f (circles), and 3d_{5/2} (stars) main lines, and the 4d⁻²4f⁸ (diamonds) and 4p⁻¹4d⁻¹4f⁸ (squares) satellites in the 3d \rightarrow 4f excitation region. Above the 3d_{5/2} threshold, the 4d, 4f, 4d⁻²4f⁸, and 4p⁻¹4d⁻¹4f⁸ cross sections have been corrected for appreciable intensity contributions by Auger electrons from decay of the 3d_{5/2} hole state.



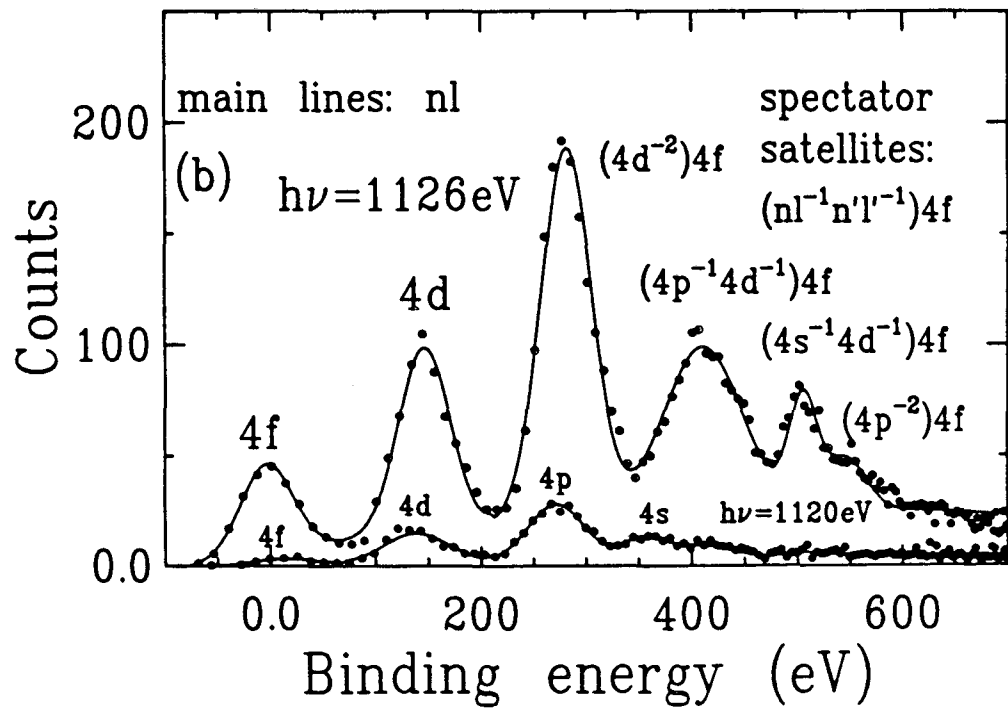
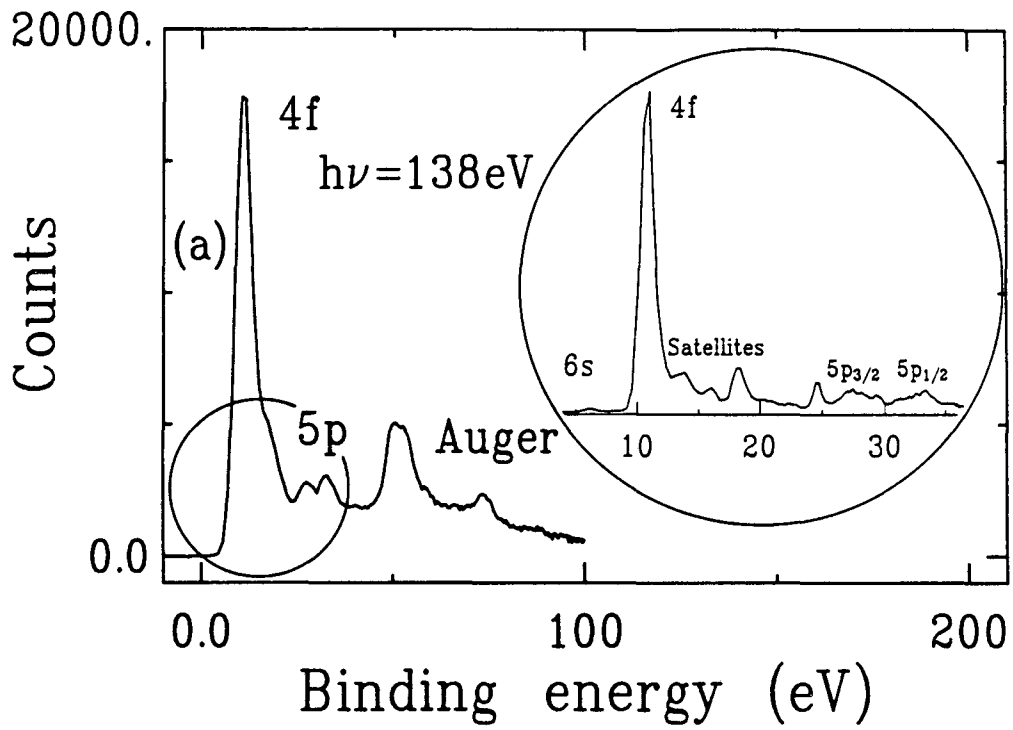
XBL 857-3035

Figure 1



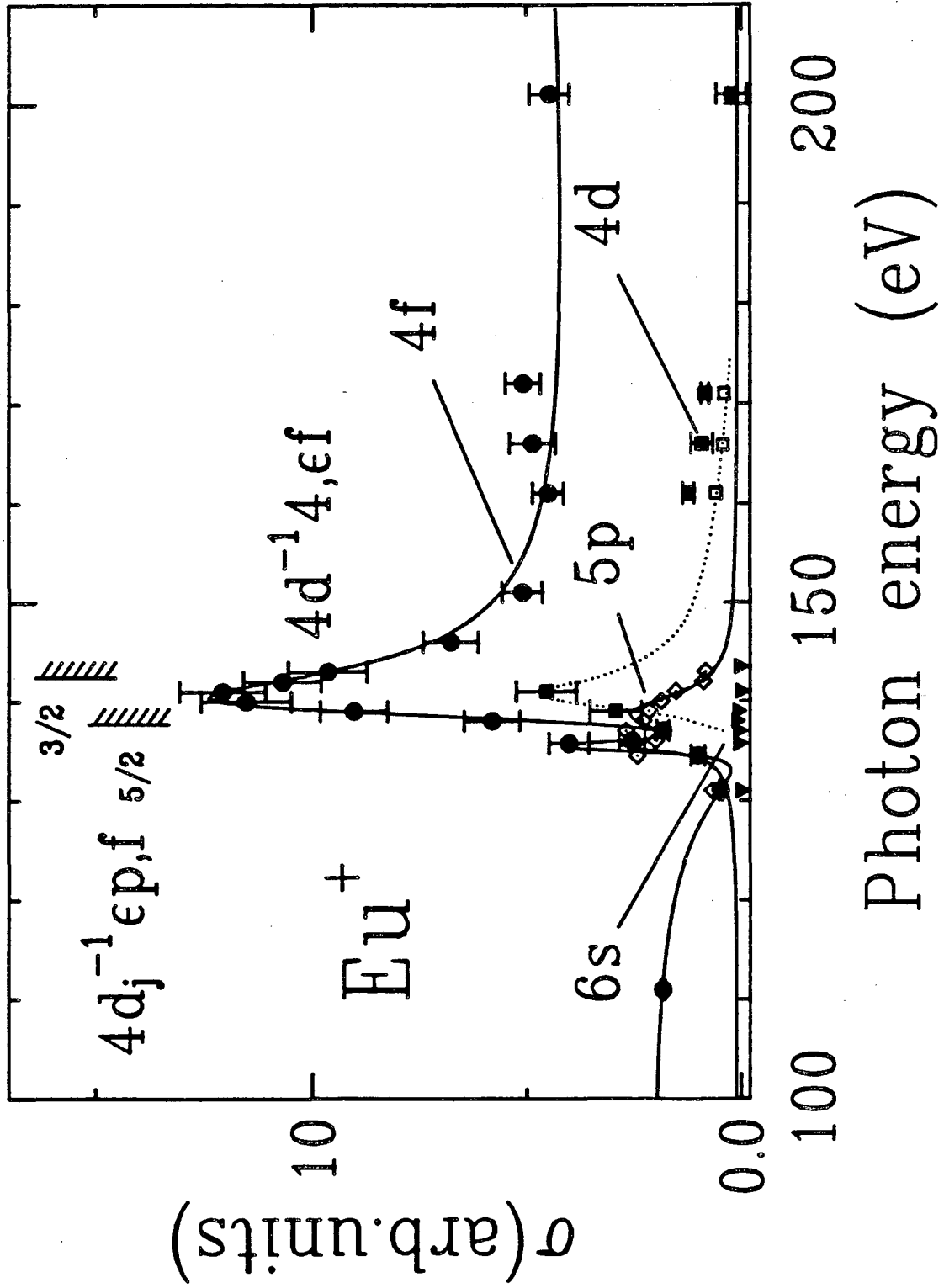
XBL 857-3036

Figure 2



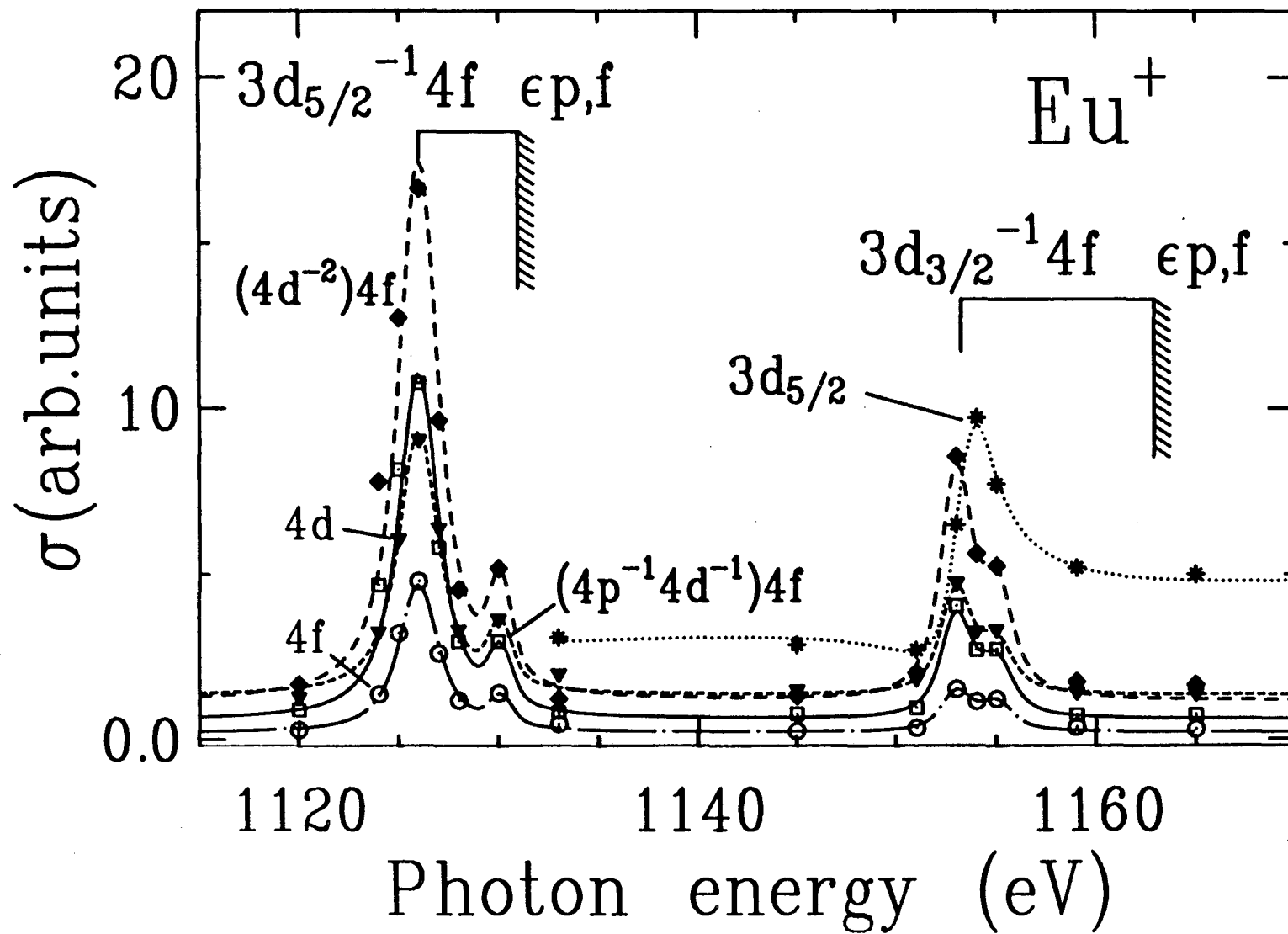
XBL 857-3037

Figure 3



XBL 857-3038

Figure 4



XBL 857-3039

Figure 5

This report was done with support from the Department of Energy. Any conclusions or opinions expressed in this report represent solely those of the author(s) and not necessarily those of The Regents of the University of California, the Lawrence Berkeley Laboratory or the Department of Energy.

Reference to a company or product name does not imply approval or recommendation of the product by the University of California or the U.S. Department of Energy to the exclusion of others that may be suitable.

*LAWRENCE BERKELEY LABORATORY
TECHNICAL INFORMATION DEPARTMENT
UNIVERSITY OF CALIFORNIA
BERKELEY, CALIFORNIA 94720*